*Progress In Electromagnetics Research Letters, Vol. 41, 193–203, 2013*

# COMPACT TUNABLE DUAL-BAND BANDPASS FILTER BASED ON SUBSTRATE INTEGRATED WAVEGUIDE AND DEFECTED GROUND STRUCTURE

**Zhu-Dan Wang***, **Feng Wei, Li Zhang, and Xiao-Wei Shi**

National Laboratory of Science and Technology on Antennas and Microwaves, Xidian University, Xi'an 710071, P. R. China

**Abstract**—A compact tunable dual-band bandpass filter (BPF) based on substrate integrated waveguide (SIW) and defected ground structure (DGS) is investigated in this paper. The second passband can be flexibly controlled by changing the dimensions of the up-down DGSs whereas the first passband is fixed. The proposed filter exhibits improved selectivity due to the introduction of four left-right DGSs generating transmission zeroes. To verify the design method, a compact dual-band filter with the second center frequency switched among 5.4 GHz, 5.8 GHz, 6.4 GHz and 6.8 GHz and the first center frequency fixed at 4.78 GHz, is designed and fabricated. The simulated and measured results are in good agreement with each other.

## 1. INTRODUCTION

Recently, substrate integrated waveguide (SIW), which is realized by metallic vias on low loss substrate through printed circuit board (PCB) or low temperature co-fired ceramic (LTCC) fabrication process, has drawn much attention to designing high-performance filters [1–6]. The SIW has similar field distribution to that of a conventional rectangular waveguide and realizes high-$Q$ factor and high power capability. Moreover, the SIW largely preserves the advantages over conventional rectangular waveguide in low cost and compact size.

With the rapid development of wireless communication systems, dual-band/multiband filters and tunable filters are drawing more attention due to their potential to significantly reduce system size and complexity. Most efforts have been focused on operating SIW to implement bandpass filters and dual mode filters [20–22]. However,

*Received 25 June 2013, Accepted 20 July 2013, Scheduled 16 August 2013*
* Corresponding author: Zhu-Dan Wang (zhdwang@stu.xidian.edu.cn).

a few works concerned about dual-band SIW filter with frequency tunability due to the difficulty in adding PIN diodes or other components.

In this study, a compact tunable dual-band SIW BPF with defected ground structure (DGS) is presented. The predicted second passband, which is switched among 5.4 GHz, 5.8 GHz, 6.4 GHz and 6.8 GHz, is obtained by changing the dimensions of the up-down DGSs. The four center frequencies of the second passband can be conveniently tuned to desired values by changing the positions of the zero ohmic resistors, so the proposed structure provides more degrees of freedom to implement tunability. The first passband is fixed at 4.78 GHz with different dimensions of the up-down DGSs. For improving the selectivity, the left-right DGSs are introduced to generate transmission zeroes and heighten the coupling degree at the input and output port of the filter. Without extra circuit, the low insertion-loss performance in the passband and compact size can be realized. To certify the proposed approach, a compact dual-band SIW filter is optimally designed, fabricated and measured. Simulations and measurements are carried out to prove the validity of this tunable filter.

## 2. DESIGN AND ANALYSIS OF PROPOSED FILTER

### 2.1. Characteristics of Substrate Integrated Waveguide with Defected Ground Structure

Figure 1(a) shows the DGS with an etched square defect on the ground plane, and its equivalent circuit is shown in Fig. 1(b). The value of equivalent inductance of DGS unit is influenced by the size of the

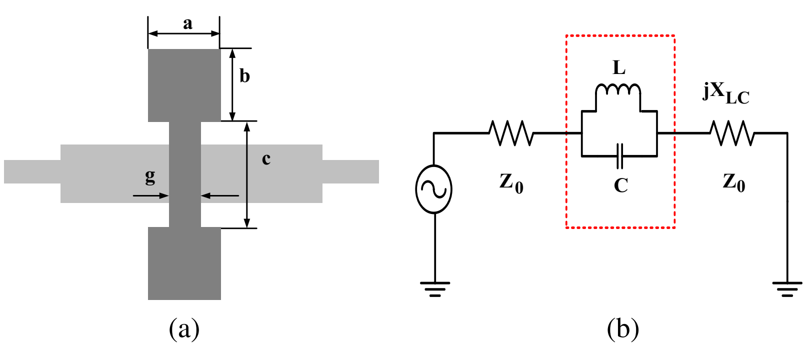


**Figure 1.** Layout schematic of (a) DGS unit cell and (b) equivalent circuit.

up-down rectangle, which can be varied by optimizing parameters $a$ and $b$. The equivalent capacitance of DGS as a function of the slot is controlled by parameter $g$.

The substrate with a thickness of 1.0 mm and relative permittivity of 2.2 is used in all of our design. The metallic vias has a diameter of 1.0 mm and a center to center spacing of 2 mm. With Ansoft's High Frequency Structure Simulator (HFSS) software, the $S$-parameters of the SIW-DGS resonator and the corresponding SIW resonator are simulated and investigated. As shown in Fig. 2, the DGS exhibits excellent stopband characteristics and slow-wave characteristics when patterned on the ground of SIW, which can be exploited to enhance selectivity by generating transmission zero and broaden stopband [13]. Moreover, the SIW and DGS can be highly integrated together and only occupy the area of a single SIW cavity, which can realize small size.

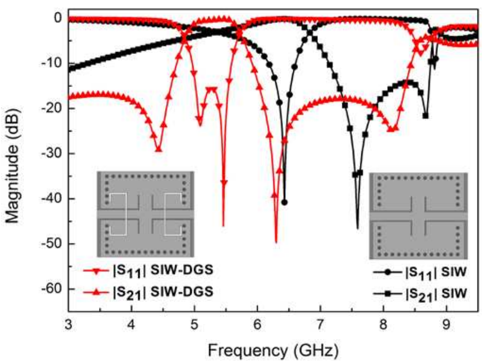


**Figure 2.** Simulated $S$-parameters corresponding to SIW-DGS and SIW cavity.

## 2.2. Design of Proposed Dual-band Structure

Figure 3 shows the layout schematic of the proposed dual-band filter. The center frequencies of the first and second passbands can be controlled independently. The first passband depends on the SIW cavity and the left-right DGSs while the second passband depends on the up-down DGSs. The gap of DGS is used to control the couplings among source and DGS resonators. The narrower the gap is, the weaker the coupling will be.

Due to the filter design methodology, the shape and fractional bandwidth of the filter is approximately determined in terms of coupling coefficients and external quality factor. The coupling

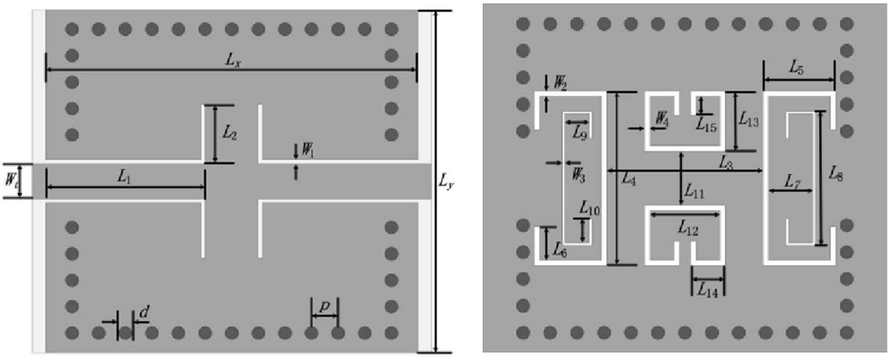


(a) (b)

**Figure 3.** Layout schematic for (a) top view and (b) bottom view of the proposed dual-band filter.

coefficients among DGS resonators and SIW cavity should belong to electric coupling, and calculated by

$$M_{ij} = \pm\left(f_{p2}^2 - f_{p1}^2\right)/\left(f_{p2}^2 + f_{p1}^2\right) \tag{1}$$

where $f_{p1}$ and $f_{p2}$ represent the lower and higher resonant frequencies, respectively. A loaded external quality factor $Q_e$ can be defined as the following equation

$$Q_e = \frac{\omega_0}{\Delta\omega_{3\,\mathrm{dB}}} \tag{2}$$

where $\omega_0$ is the resonant frequency and $\Delta\omega_{3\,\mathrm{dB}}$ the bandwidth for which the attenuation for $S_{21}$ is up to 3 dB from that at resonance.

The co-planar waveguide (CPW) is used to excite the SIW cavity and DGS resonators [13, 14]. The DGS resonators can be moved longitudinally so as to minimize the coupling between DGSs and SIW cavity, which has a little effect on the coupling between DGS resonators. The source-load coupling is taken as the magnetic case, which is contributed by the maximum magnetic field at each ends of the probes [13]. The source-load coupling becomes stronger with $L_1$ increasing, and the transmission zero located at high stopband is moved towards the passband. Either $L_1$ or $L_2$ is used to control the external $Q$-factor of SIW cavity. As shown in Fig. 4, the larger $L_1$ or $L_2$ is, the smaller the external $Q$-factor of SIW will be.

From experimental demonstrations, it can be found that the variation of the second passband with the dimensions of the up-down DGSs has almost no effect on the first passband. As shown in Fig. 5, the size of the up-down DGSs becomes smaller as $L_{15}$ decreases, resulting in a higher center frequency $f_{o2}$. In this design,

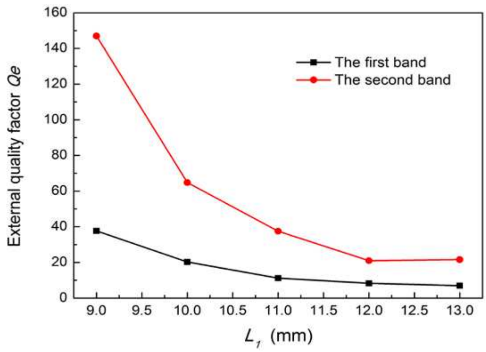


**Figure 4.** External quality factor versus the configuration of $L_1$.

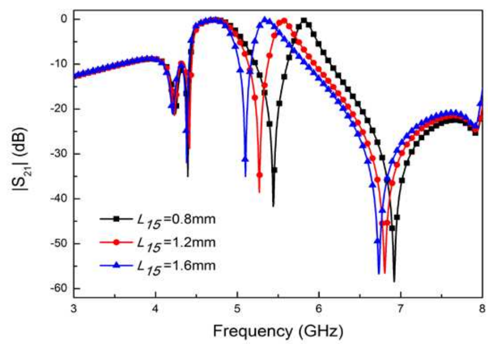


**Figure 5.** Simulated $S_{21}$-parameters for different values of $L_{15}$.

an introduction of the left-right DGSs strengthens the source-load coupling and generates additional transmission zero located at the low stopband. As presented in Fig. 6, the source-load coupling becomes stronger with increasing $L_3$, and the transmission zero located at low stopband moves towards the passband. However, the variation of $L_3$ has little effect on the transmission zero at the high stopband.

## 2.3. Implementation of Tunable Dual-band Filter

Figure 7 shows schematic drawing of changing the dimensions of the up-down DGSs based on six switches. According to different states of the six switches, they are categorized into four different combinations for all-on, $S_{W1}$-off, $S_{W2}$-off and $S_{W3}$-off, and the corresponding $S$-parameters are shown in Fig. 8. In practical application, zero ohmic resistors are used as connection switches.

As shown in Fig. 8, it can be found that the center frequency of

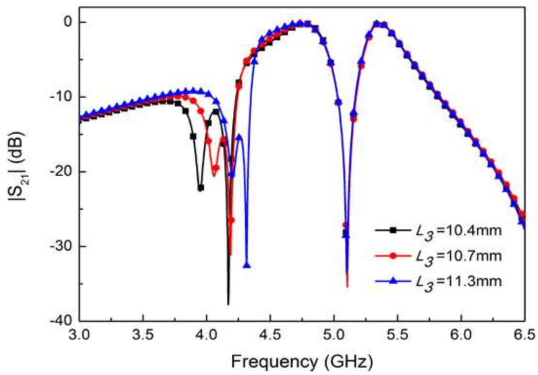


**Figure 6.** Simulated $S_{21}$-parameters for different values of $L_3$.

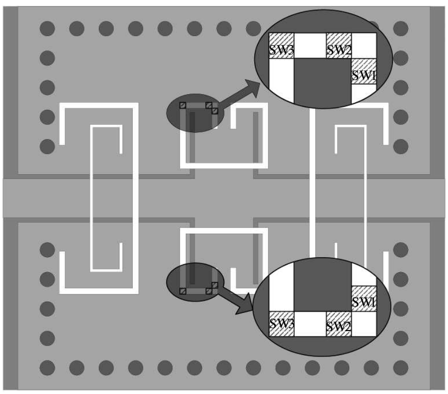


**Figure 7.** Layout of the proposed tunable filter.

the second passband is switched among 5.4 GHz, 5.8 GHz, 6.4 GHz and 6.8 GHz with the first center frequency fixed at 4.78 GHz. With the positions of the six switches changed, four other frequencies will be obtained. Therefore, the proposed structure provides more degrees of freedom to implement tunability. The developed tunable dual-band filter incorporates two passbands within a single filter structure without introducing extra losses, yet with a compact size achieved. Additionally, it greatly simplifies the assembly and integration of the resonators, resulting in substantial reduction in time and costs.

In this design, all the dimensions are selected as follows: $L_x = 30$ mm, $L_y = 26$ mm, $L_1 = 11.7$ mm, $L_2 = 4.5$ mm, $L_3 = 11.6$ mm, $L_4 = 12.2$ mm, $L_5 = 5.4$ mm, $L_6 = 2.5$ mm, $L_7 = 3.3$ mm, $L_8 = 9.8$ mm, $L_9 = 2.2$ mm, $L_{10} = 2$ mm, $L_{11} = 4$ mm, $L_{12} = 6$ mm,

$L_{13} = 4.5\,\mathrm{mm}$, $L_{14} = 2.575\,\mathrm{mm}$, $L_{15} = 1.8\,\mathrm{mm}$, $W_t = 2.65\,\mathrm{mm}$, $W_1 = 0.3\,\mathrm{mm}$, $W_2 = 0.4\,\mathrm{mm}$, $W_3 = 0.4\,\mathrm{mm}$, $W_4 = 0.2\,\mathrm{mm}$, $d = 1\,\mathrm{mm}$, $p = 2\,\mathrm{mm}$.

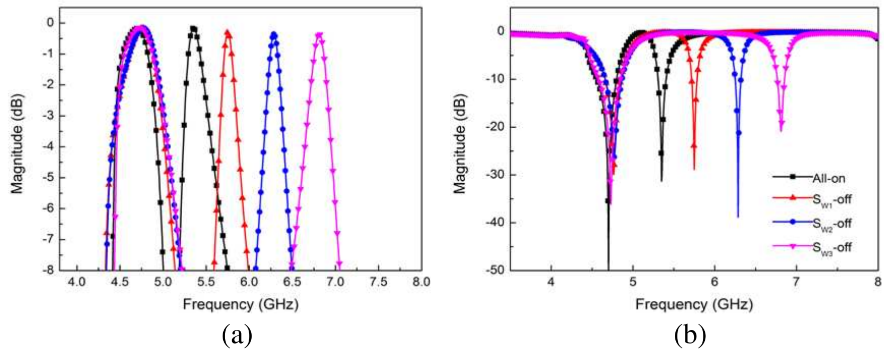


**Figure 8.** Simulated results of the filter. (a) Insertion loss. (b) Return loss.

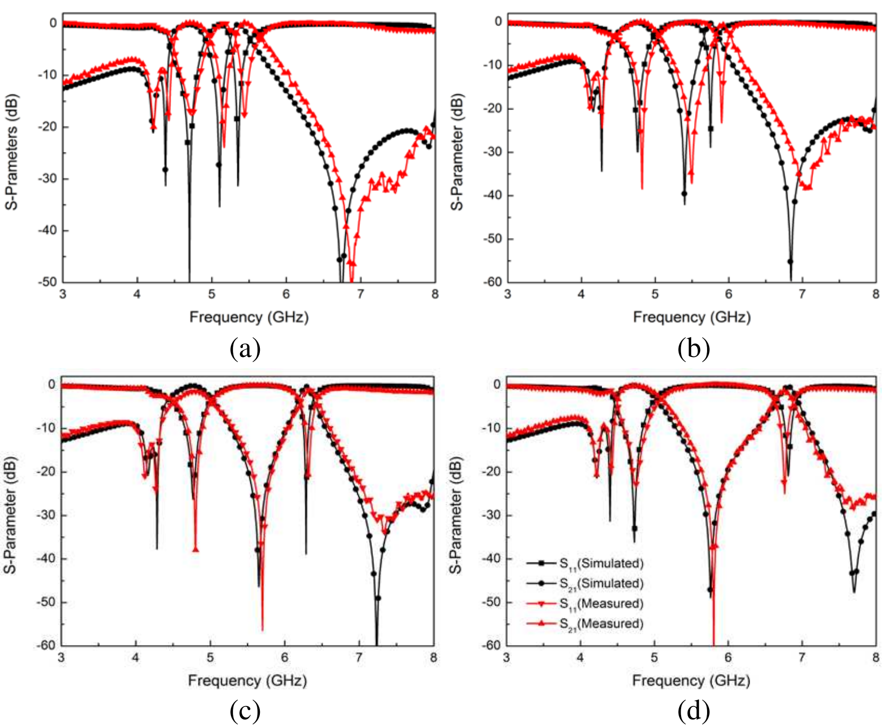


**Figure 9.** Simulated and measured results of proposed filter. (a) All-on. (b) $S_{W1}$-off. (c) $S_{W2}$-off. (d) $S_{W3}$-off.

## 3. RESULTS AND DISCUSSION

Finally, the simulations are carried out by Ansoft HFSS version 13, and the measured results are gained from Agilent vector network analyzer N5230A.

Figure 9 shows the comparison between the simulated and measured results. The fabricated filter has the second passband switched at 5.4/5.8/6.4/6.8 GHz, and the 3 dB fractional bandwidths of which are 5.4/3.3/3.1/3.8%. The measured in-band minimum insertion losses of all configurations are from 0.32 dB to 1.8 dB, which contains the loss from the connectors, while in-band return losses are better than −20 dB. The first passband is fixed at 4.78 GHz, and the 3 dB fractional bandwidth of which is around 550 MHz. Transmission

**Table 1.** Filter characteristics versus configuration of the switches.

| | Switch operation | | | Lower 3 dB Cutoff Frequency (GHz) | | Upper 3 dB Cutoff Frequency (GHz) | |
|---|---|---|---|---|---|---|---|
| | $S_{W1}$ | $S_{W2}$ | $S_{W3}$ | 1st passband | 2nd passband | 1st passband | 2nd passband |
| State 1 | on | on | on | 4.45 | 5.24 | 4.91 | 5.53 |
| State 2 | off | on | on | 4.45 | 5.66 | 4.98 | 5.85 |
| State 3 | on | off | on | 4.45 | 6.19 | 5.01 | 6.38 |
| State 4 | on | on | off | 4.47 | 6.67 | 5.01 | 6.93 |
| | Switch operation | | | 3 dB Bandwidth (%) | | Maximum Insertion Loss (dB) | |
| | $S_{W1}$ | $S_{W2}$ | $S_{W3}$ | 1st passband | 2nd passband | 1st passband | 2nd passband |
| State 1 | on | on | on | 16.7 | 5.4 | 0.38 | 0.32 |
| State 2 | off | on | on | 25.4 | 3.3 | 0.34 | 0.35 |
| State 3 | on | off | on | 11.7 | 3.1 | 1.8 | 1.3 |
| State 4 | on | on | off | 11.4 | 3.8 | 0.5 | 1.6 |

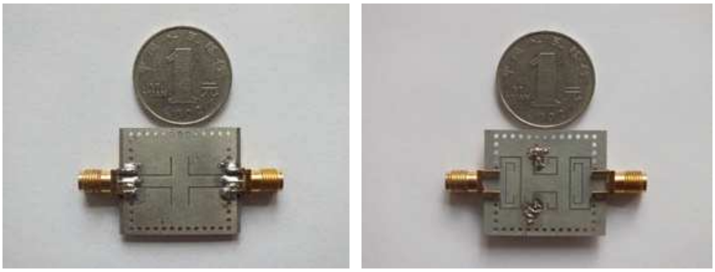

(a) (b)

**Figure 10.** Photographs for (a) top view and (b) bottom view of the fabricated filter.

zeroes are generated by left-right DGSs, which can improve passband selectivity and result in a high isolation. The deviations of the measurements from the simulations are expected mainly due to the reflections from the connectors and the finite substrate. Fig. 10 shows the photograph of the fabricated tunable dual-band BPF. The overall size is about 26 mm × 30 mm. Table 1 shows the filter characteristics versus configuration of the switches.

## 4. CONCLUSION

In this paper, a compact tunable dual-band bandpass filter based on SIW and DGS is presented. The center frequency of the second passband can be conveniently tuned to desired values by controlling the DGS dimensions. In addition, there are four transmission zeroes on sides of passbands, which improves the skirt selectivity. The design method can be applicable to selectable multiband applications. A demonstration filter has been implemented. The good performance, planar structure and compact size make it attractive for wireless communications.

## ACKNOWLEDGMENT

This work was supported by the Fundamental Research Funds for the Central Universities (K50511020013) and the National Natural Science Foundation of China under Grant 61101069.

## REFERENCES

1. Xu, Z. and H. Xia, "Miniaturized multilayer dual-mode substrate integrated waveguide filter with multiple transmission zeros,"

*Progress In Electromagnetics Research*, Vol. 139, 627–642, 2013.
2. Li, D., C. Tong, J. Bao, P. Peng, and D. Yu, "A novel bandpass filter of substrate integrated waveguide (SIW) based on S-shaped EBG," *Progress In Electromagnetics Research Letters*, Vol. 36, 191–200, 2013.
3. Zhang, Q. L., W. Y. Yin, S. He, and L. S. Wu, "Evanescent-mode substrate integrated waveguide (SIW) filters implemented with complementary split ring resonators," *Progress In Electromagnetics Research*, Vol. 111, 419–432, 2011.
4. Deslandes, D. and K. Wu, "Accurate modeling, wave mechanism, and design consideration of a substrate integrated waveguide," *IEEE Trans. on Microw. Theory and Tech.* Vol. 54, No. 6, 2516–2526, Jun. 2006.
5. Hao, Z. C., W. Hong, J. X. Chen, X. P. Chen, and K. Wu, "Compact super-wide bandpass substrate integrated waveguide (SIW) filters," *IEEE Trans. on Microw. Theory and Tech.*, Vol. 53, No. 9, 2968–2977, Sep. 2005.
6. Zhang, Y. L., W. Hong, K. Wu, J. X. Chen, and H. J. Tang, "Novel substrate integrated waveguide cavity filter with defected ground structure," *IEEE Trans. on Microw. Theory and Tech.*, Vol. 53, 1280–1286, 2005.
7. Leszczynska, N., L. Szydlowski, and M. Mrozowski, "A novel synthesis technique for microwave bandpass filters with frequency-dependent couplings," *Progress In Electromagnetics Research*, Vol. 137, 35–50, 2013.
8. Deng, Z., W. Jiang, S. Gong, Y. Xu, and Y. Zhang, "A new method for broadening bandwidths of circular polarized microstrip antennas by using DGS parasitic split-ring resonators," *Progress In Electromagnetics Research*, Vol. 136, 739–751, 2013.
9. Taher, H., "A simplified equivalent circuit model for defected ground structures in planar transmission lines," *Progress In Electromagnetics Research Letters*, Vol. 29, 157–166, 2012.
10. Liu, J., K. P. Esselle, S. G. Hay, and S. S. Zhong, "Study of an extremely wideband monopole antenna with triple band-notched characteristics," *Progress In Electromagnetics Research*, Vol. 123, 143–158, 2012.
11. Lim, P. L. and K. M. Lum, "A novel bandpass filter design using E-shaped resonator and dual square-loop defected ground structure," *PIERS Proceedings*, 610–614, Kuala Lumpur, Malaysia, Mar. 27–30, 2012.
12. Ghazali, A. N. and S. Pal, "Analysis of a small UWB filter

with notch and improved stopband," *Progress In Electromagnetics Research Letters*, Vol. 34, 147–156, 2012.

13. Wei, S., W.-Y. Yin, and X.-W. Sun, "Compact substrate integrated waveguide (SIW) filter with defected ground structure," *IEEE Microwave and Wireless Components Letters*, Vol. 21, No. 2, 83–85, 2011.
14. Wang, Z.-D., F. Wei, L. Zhang, and X.-W. Shi, "Design of dual-band bandpass SIW filter with DGS," *2012 International Conference on Microwave and Millimeter Wave Technology*, 1–3, Piscataway, NJ, USA, May 5–8, 2012.
15. Huang, Y., Z. Shao, and L. Liu, "A substrate integrated waveguide bandpass filter using novel defected ground structure shape," *Progress In Electromagnetics Research*, Vol. 135, 201–213, 2013.
16. Chu, H. and X. Q. Shi, "Compact ultra-wideband bandpass filter based on SIW and DGS technology with a notch band," *Journal of Electromagnetic Waves and Applications*, Vol. 25, No. 4, 589–596, 2011.
17. He, Z., J. Cai, Z. Shao, X. Li, and Y. Huang, "A novel power divider integrated with SIW and DGS technology," *Progress In Electromagnetics Research*, Vol. 139, 289–301, 2013.
18. Jedrzejewski, A., N. Leszczynska, L. Szydlowski, and M. Mrozowski, "Zero-pole approach to computer aided design of in-line SIW filters with transmission zeros," *Progress In Electromagnetics Research*, Vol. 131, 517–533, 2012.
19. Wang, J., H. Ning, Q. Xiong, M. Li, and L.-F. Mao, "A novel miniaturized dual-band bandstop filter using dual-plane defected structures," *Progress In Electromagnetics Research*, Vol. 134, 397–417, 2013.
20. Zhang, Q., B.-Z. Wang, W.-Y. Yin, and L.-S. Wu, "Design of a miniaturized dual-band double-folded substrate integrated waveguide bandpass filter with controllable band-widths," *Progress In Electromagnetics Research*, Vol. 136, 211–223, 2013.
21. Chen, L.-N., Y.-C. Jiao, Z. Zhang, F.-S. Zhang, and Y.-Y. Chen, "Miniaturized dual-mode substrate integrated waveguide (SIW) band-pass filters loaded by double/single T-shaped structures," *Progress In Electromagnetics Research Letters*, Vol. 29, 65–74, 2012.
22. Liu, C. and K. Huang, "A compact substrate integrated waveguide band-pass filter," *PIERS Proceedings*, 1135–1138, Cambridge, USA, Jul. 5–8, 2010.